The Circular Homogeneous-Ferrite Microwave Cirulator—An Asypmtotic Green's Function and Impedance Analysis

Jeffrey L. Young, *Senior Member, IEEE,* and James W. Sterbentz

***Abstract*—A detailed analysis of the circular, homogeneous ferrite microwave circulator is provided. Particular emphasis is on the circulator's Green's function and the impact of the asymptotic term within the Green's function on convergence, data quality, and design methodology. The asymptotic term is shown to be logarithmic, which suggests that the Green's function is weakly singular when the source and observation points occupy the same location. With the Green's function properly understood, two techniques—one analytical and one numerical—are then offered to integrate that function in order to obtain Z-parameter data and, subsequently, S-parameter data. Data are provided to show rapid convergence of all parameters of interest. A small coupling angle approximation is then given for the Z-parameters and, from that approximation, a first-order design equation is obtained that relates the coupling angle to circulator radius. A circulator design example is presented and compared to a design associated with the Wu and Rosenbaum method; the comparison substantiates the small coupling angle approximation and design formula.**

***Index Terms*—Asymptotic analysis, circulator, ferrite, Green's function.**

I. Introduction

THERE EXISTS considerable interest in the design, analysis, and modeling of ferrite devices within the microwave circuits community [1]. This interest is spawned, in part, from the role that ferrite devices have in directing energy to specific destinations within a circuit (i.e., the circulator and isolator), shifting the phase of an electromagnetic wave, or filtering the frequency spectrum of an electromagnetic signal. In the past, these devices were constructed using bulky external magnets to maintain material magnetization; recently, with the advent of new ferrite materials and thick-film processes, integrated self-biased ferrites are now possible [2], [3].

In this paper, we are interested in the small-signal analysis of the cylindrical circulator, as initially considered by Bosma [4] and by Davies and Cohen [5]. Their analysis is based upon the assumption that the circulator can be modeled as a closed cylindrical cavity whose surfaces are a mixture of perfect magnetic conductors (PMCs) and perfect electric conductors (PECs); the cavity is assumed to be filled with a homogeneous axially biased anisotropic ferrite. When the cavity is excited by a uniform axially directed electric current sheet that exists along the vertical side of the cavity, the spatial variation in the electromagnetic fields is two-dimensional. The advantage of this approach is found in the simple construction of a scalar integral equation that relates axial electric intensity to azimuthal magnetic intensity.

This integral equation has been the subject of many papers and has been used to: 1) determine narrow-band design equations for the circulator [4]; 2) describe the circulator's physical operation in terms of two counter-opposing azimuthal modes [6]; 3) provide a design procedure for wide-band operation [7]; 4) characterize the behavior of the circulator for negative permeability [8]; and 5) analyze the various loss mechanisms within the circulator [9]–[11]. In each of these cases, knowledge of Bosma's original two-dimensional Green's function, which is the kernel of the integral equation, is required. Although the Bosma Green's function, as it shall be called, has been correctly derived in terms of an infinite series of azimuthal modes, the singularity and asymptotic nature of this Green's function has not been adequately investigated. In this paper, such an investigation is provided.

By understanding the asymptotic and singular nature of the Bosma Green's function, we demonstrate how an accurate evaluation of the circulator's Z- and S-parameters can be made. Specifically, the Z-parameters, which are obtained by integrating the Green's function over some portion of the sidewall of the cavity, are cast in terms of a rapidly converging series and an asymptotic term. The asymptotic term can be evaluated by using Taylor series techniques or by using Gauss-quadrature numerical methods. If Taylor analysis is employed, we show how the asymptotic impedances, particularly the asymptotic self-impedance, can be utilized to assist in the design of the circulator in order to achieve perfect circulation. To this end, a simple first-order design formula that relates coupling angle to disk radius is derived. To validate the formula, a design example is provided and S-parameter data for the same are plotted. The data clearly manifest the match, isolation, and insertion-loss conditions that are expected of a circulator.

It has been noted in the literature that Bosma's model excludes the important effect of the demagnetizing field, which creates a ferrite that is highly inhomogeneous in the radial direction [12]. Since the circular ferrite is typically azimuthally homogeneous, however, it is possible to model the inhomogeneous effect by creating a radially stratified ferrite that is a discretization of the continuous ferrite and to develop a recursive Green's function for the same [13]–[15]. It is surmised that the

Manuscript received October 16, 2002; revised March 5, 2003. This work was supported by the Office of Naval Research under Contract N000140110941.

J. L. Young is with the Department of Electrical and Computer Engineering, University of Idaho, Moscow, ID 83844-1023 USA.

J. W. Sterbentz is with the Idaho National Engineering and Environmental Laboratory, Idaho Falls, ID 83415 USA.

Digital Object Identifier 10.1109/TMTT.2003.815268

analysis provided herein could be applied to this Green's function as well; the ease or difficulty of making such an application is the subject of future work.

II. Formulation

The approach considered herein, as introduced by Bosma [4], is to assume that the circulator can be modeled as a closed cylindrical cavity that is homogeneously filled with an axially biased ferrite material. (The axial direction corresponds to the Cartesian z-axis.) The top and bottom surfaces are considered to be PECs; the sidewall surfaces are assumed to be PMCs. The radius and height of the cavity are a and h, respectively. If the cavity is excited by a uniform line source that extends from the bottom surface to the top surface, field variations in the axial direction are absent, which implies that the electromagnetic fields are two-dimensional in the radial and azimuthal directions (i.e., r and ϕ, respectively).

Per Bosma, a Green's function $G(\phi,\phi')$ is sought that relates the small-signal electric intensity E_z to the small-signal magnetic intensity H_ϕ on the walls of the cavity (i.e., $r=a$) in terms of the following integral equation:

$$E_z(\phi)=\int_{-\pi}^{\pi} G(\phi,\phi')H_\phi(\phi')d\phi'. \tag{1}$$

The derivation of the Green's function $G(\phi,\phi')$ has been provided in several sources (e.g., [4]) and, hence, it suffices to simply state its form. For purposes of future mathematical manipulations, that form is given in terms of modified Bessel functions per Neidert and Phillips [9] as follows:

$$G(\phi,\phi')=\frac{Z_f}{2\pi}\frac{I_0(\gamma_f a)}{I_0'(\gamma_f a)}+S_1+S_2 \tag{2}$$

where

$$S_1=\frac{Z_f}{2\pi}\sum_{n=1}^{\infty}\frac{I_n(\gamma_f a)e^{jn(\phi-\phi')}}{I_n'(\gamma_f a)+(n\kappa/\mu_f)\,I_n(\gamma_f a)/(\gamma_f a)} \tag{3}$$

and

$$S_2=\frac{Z_f}{2\pi}\sum_{n=1}^{\infty}\frac{I_n(\gamma_f a)e^{-jn(\phi-\phi')}}{I_n'(\gamma_f a)-(n\kappa/\mu_f)\,I_n(\gamma_f a)/(\gamma_f a)}. \tag{4}$$

Here, $I_n(z)$ is the modified Bessel function of the first kind of argument z and $I_n'(z)$ is its derivative with respect to z. The secondary parameters Z_f and γ_f are the wave impedance and wavenumber of the ferrite, respectively, $Z_f=\sqrt{\mu_e/\epsilon_f}$ and where $\gamma_f=\omega\sqrt{-\mu_e\epsilon_f}$, where $\mu_e=(\mu_f^2-\kappa^2)/\mu_f$. Here, μ_f and κ are elements of the Polder matrix [16]. To assure decaying solutions and passive material status, regardless of the sign of μ_e, the branch cuts are chosen such that $\mathrm{Re}\{\gamma_f\}>0$ and $\mathrm{Re}\{Zf\}>0$. By expressing the branch cut of γ_f as such, we avoid the need to express $G(\phi,\phi')$ in terms of $J_n(z)$, which is the Bessel function of the first kind.

To understand the convergence properties of either S_1 or S_2, note that, for large n

$$\frac{I_n(\gamma_f a)}{I_n'(\gamma_f a)\pm(n\kappa/\mu_f)\,I_n(\gamma_f a)/(\gamma_f a)}\to\frac{\gamma_f a}{n\,(1\pm\kappa/\mu_f)} \tag{5}$$

per the asymptotic theory of Bessel functions [17]. As expected, the Green's function converges at the rate of $1/n$. To improve convergence, the asymptotic term is removed from the summation and separately summed in closed form [18]. Using the result from Wheelon [19] that

$$\sum_{n=1}^{\infty}\frac{e^{\pm jn(\phi-\phi')}}{n}=-\ln\left(1-e^{\pm j(\phi-\phi')}\right) \tag{6}$$

we replace (2) with

$$G(\phi,\phi')=\frac{Z_f}{2\pi}\left[\frac{I_0(\gamma_f a)}{I_0'(\gamma_f a)}+S_1'+S_2'\right]+G^a(\phi,\phi') \tag{7}$$

where

$$S_1'=\sum_{n=1}^{\infty}A_n e^{jn(\phi-\phi')} \tag{8}$$

and

$$S_2'=\sum_{n=1}^{\infty}B_n e^{-jn(\phi-\phi')}. \tag{9}$$

Here

$$A_n=\frac{I_n(\gamma_f a)}{I_n'(\gamma_f a)+(n\kappa/\mu_f)\,I_n(\gamma_f a)/(\gamma_f a)}-\frac{\gamma_f a}{n\,(1+\kappa/\mu_f)} \tag{10}$$

and

$$B_n=\frac{I_n(\gamma_f a)}{I_n'(\gamma_f a)-(n\kappa/\mu_f)\,I_n(\gamma_f a)/(\gamma_f a)}-\frac{\gamma_f a}{n\,(1-\kappa/\mu_f)}. \tag{11}$$

Finally, $G^a(\phi,\phi')$ is the asymptotic term associated with $G(\phi,\phi')$ and is given by

$$G^a(\phi,\phi')=-\frac{Z_f\gamma_f a}{2\pi}\left[\frac{\ln\left(1-e^{j(\phi-\phi')}\right)}{1+\left(\frac{\kappa}{\mu_f}\right)}+\frac{\ln\left(1-e^{-j(\phi-\phi')}\right)}{1-\left(\frac{\kappa}{\mu_f}\right)}\right]. \tag{12}$$

As expected, the singular nature of the Green's function is manifested in $G^a(\phi,\phi')$, which is implicitly present within the original Bosma Green's function of (2), i.e., the summations within (2) become logarithmically divergent whenever the source and observation points occupy the same location. (This effect was also observed by Schloemann and Blight [8] for the special case when $\mu_e=0$.) However, even if ϕ and ϕ' are not the same, but are close to each other, the implicit logarithmic nature of (2) leads to series that are technically convergent, but computationally slow to converge. This slowness-to-converge attribute is due to the $1/n$ convergence rate of S_1 and S_2. However, by subtracting the asymptotic terms from the series, as was done in (8) and (9), we create series that converge at the rate of $1/n^2$. For computational purposes, this type of convergence is sufficiently rapid and, as the numerical results reveal, extremely tight convergence can be achieved in 5-15 terms.

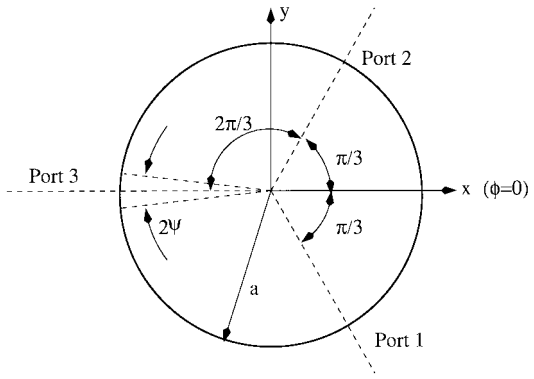

Fig. 1. Port definitions for the cavity.

With the Green's function of (7) so developed, it now behooves us to consider the impedance effects of the cavity. We do so by regarding the cavity as a three-port device, whose ports are geometrically located per the diagram of Fig. 1. The ports are regarded as locations where either current sources are impressed or where open circuit voltage calculations are made. The open-circuit nature of the ports follows directly from the PMC boundary condition associated with the cavity. The defining integral equation of (1) reveals that $G(\phi,\phi')$ is a transimpedance function that relates the impressed current sources on the azimuthal wall of the cavity (i.e., H_ϕ) to the voltage response on the same (i.e., E_z). Due to the assumed small-signal linearity of the ferrite, it follows that E_z and H_ϕ are related to each other at the ports by means of the impedance parameters Z_{ij}, e.g.,

$$Z_{11} = \int_{(-(\pi/3)-\psi)}^{(-(\pi/3)+\psi)} G(-(\pi/3),\phi')\,d\phi'. \tag{13}$$

Likewise

$$Z_{21} = \int_{(-(\pi/3)-\psi)}^{(-(\pi/3)+\psi)} G((\pi/3),\phi')\,d\phi' \tag{14}$$

and

$$Z_{31} = \int_{(-(\pi/3)-\psi)}^{(-(\pi/3)+\psi)} G(\pi,\phi')d\phi' \tag{15}$$

where $G(\phi,\phi')$ is given by (7). Similar definitions can be provided for the remaining impedance parameters. However, such a provision is not necessary since the symmetry of the Green's function leads to the following conclusions: $Z_{21}=Z_{32}=Z_{13}$, $Z_{31}=Z_{23}=Z_{12}$, and $Z_{11}=Z_{22}=Z_{33}$.

The integration of (13)–(15) is trivial, except for the logarithmic terms associated with $G^a(\phi,\phi')$, which are integrable, even though they are singular at $\phi=\phi'$. The integration of G^a is possible in one of two ways. The first way is to integrate it numerically using Gauss-quadrature techniques that employ a mixture of polynomials and natural logarithms as basis functions [20]. This is numerically easy to do, but provides no impedance information associated with G^a. The second way is to approximate the integral using small argument approximations, as provided in the Appendix. From the information located in the Appendix

$$Z_{11} = \left(\frac{Z_f\psi}{\pi}\right)\frac{I_0(\gamma_f a)}{I_0'(\gamma_f a)} + \frac{Z_f}{\pi}\sum_{n=1}^{\infty}(A_n+B_n)\frac{\sin(n\psi)}{n} - Z_{11}^a \tag{16}$$

where

$$Z_{11}^a = \frac{Z_f\gamma_f a}{2\pi}\left[\frac{M_{11}^+}{1+\dfrac{\kappa}{\mu_f}} + \frac{M_{11}^-}{1-\dfrac{\kappa}{\mu_f}}\right] \tag{17}$$

which is the asymptotic term. Expressions for M_{11}^+ and M_{11}^- are given by (39) of the Appendix. Likewise,

$$\begin{aligned} Z_{21} = {} & \left(\frac{Z_f\psi}{\pi}\right)\frac{I_0(\gamma_f a)}{I_0'(\gamma_f a)} \\ & + \frac{Z_f}{\pi}\sum_{n=1}^{\infty}\left(A_n e^{((2jn\pi)/3)} + B_n e^{-((2jn\pi)/3)}\right)\frac{\sin(n\psi)}{n} \\ & - Z_{21}^a \end{aligned} \tag{18}$$

and

$$\begin{aligned} Z_{31} = {} & \left(\frac{Z_f\psi}{\pi}\right)\frac{I_0(\gamma_f a)}{I_0'(\gamma_f a)} \\ & + \frac{Z_f}{\pi}\sum_{n=1}^{\infty}\left(A_n e^{((4jn\pi)/3)} + B_n e^{-((4jn\pi)/3)}\right)\frac{\sin(n\psi)}{n} \\ & - Z_{31}^a. \end{aligned} \tag{19}$$

Here

$$Z_{21}^a = \frac{Z_f\gamma_f a}{2\pi}\left[\frac{M_{21}^+}{1+\dfrac{\kappa}{\mu_f}} + \frac{M_{21}^-}{1-\dfrac{\kappa}{\mu_f}}\right] \tag{20}$$

and

$$Z_{31}^a = \frac{Z_f\gamma_f a}{2\pi}\left[\frac{M_{31}^+}{1+\dfrac{\kappa}{\mu_f}} + \frac{M_{31}^-}{1-\dfrac{\kappa}{\mu_f}}\right]. \tag{21}$$

Expressions for M_{21}^+, M_{21}^-, M_{31}^+, and M_{31}^- are also provided in the Appendix.

To obtain useful design information, we now explore the small coupling angle case. Let N be the number of terms required to achieve adequate convergence. Moreover, if $N\psi \ll 1$, we may approximate (16), (18), and (19) with the following:

$$Z_{11} \approx \frac{Z_f\psi}{\pi}\left[\frac{I_0(\gamma_f a)}{I_0'(\gamma_f a)} + \sum_{n=1}^{N}(A_n+B_n)\right] - Z_{11}^a \tag{22}$$

$$\begin{aligned} Z_{21} \approx {} & \frac{Z_f\psi}{\pi}\frac{I_0(\gamma_f a)}{I_0'(\gamma_f a)} \\ & + \frac{Z_f\psi}{\pi}\sum_{n=1}^{N}\left(A_n e^{((2jn\pi)/3)} + B_n e^{-((2jn\pi)/3)}\right) - Z_{21}^a \end{aligned} \tag{23}$$

and

$$Z_{31} \approx \frac{Z_f\psi}{\pi}\frac{I_0(\gamma_f a)}{I_0'(\gamma_f a)} + \frac{Z_f\psi}{\pi}\sum_{n=1}^{N}\left(A_n e^{((4jn\pi)/3)} + B_n e^{-((4jn\pi)/3)}\right) - Z_{31}^a. \tag{24}$$

These equations suggest that the $\sin(n\psi)/n$ term in (16), (18), and (19) does not accelerate convergence when ψ is small, as it might first appear upon casual inspection. (In the case of Wu and Rosenbaum [7], the term $\sin^2 n\psi/(n^2\psi)$ in (9) also contributes nothing to the initial convergence rate for small coupling angles since $\sin^2 n\psi/(n^2\psi) \approx \psi$). As for the asymptotic terms, the results from (17), (20), and (21) and the small coupling angle results from the Appendix suggest that

$$Z_{11}^a \approx \frac{Z_f\psi}{\pi}(2\gamma_f a)\left[\frac{(\ln\psi - 1)}{1-\left(\frac{\kappa}{\mu_f}\right)^2}\right] \tag{25}$$

$$Z_{21}^a \approx \frac{Z_f\psi}{\pi}(\gamma_f a)\left[\frac{1+j\left(\frac{\kappa}{\mu_f}\right)}{1-\left(\frac{\kappa}{\mu_f}\right)^2}\right] \tag{26}$$

$$Z_{31}^a \approx \frac{Z_f\psi}{\pi}(\gamma_f a)\left[\frac{1-j\left(\frac{\kappa}{\mu_f}\right)}{1-\left(\frac{\kappa}{\mu_f}\right)^2}\right]. \tag{27}$$

Through these small coupling angle approximations, the impact of ψ on the open-circuit impedances is clearly seen: all open-circuit impedances are approximately proportional to ψ, except for Z_{11}^a, which is proportional to $\psi(\ln\psi - 1)$.

The classical design methodology of a circulator has been articulated by Wu and Rosenbaum [7]. We now consider the special case of that design when the coupling angle is small. With this in mind and for purposes of future manipulations, let $Z_{11} = jX_{11}$, where

$$X_{11} = \frac{Z_f\psi}{\pi}\left[f_{11}\left(\psi_f a, \frac{\kappa}{\mu_f}\right) - (\ln\psi - 1)f_{11}^a\left(\psi_f a, \frac{\kappa}{\mu_f}\right)\right]. \tag{28}$$

From (22), (25), and (28), it follows that

$$f_{11} \approx -j\left[\frac{I_0(\gamma_f a)}{I_0'(\gamma_f a)} + \sum_{n=1}^{N}(A_n + B_n)\right] \tag{29}$$

and

$$f_{11}^a \approx -\frac{2j\gamma_f a}{1-\left(\frac{\kappa}{\mu_f}\right)^2}. \tag{30}$$

Here, f_{11} and f_{11}^a are functions of $\gamma_f a$ and $\kappa/\mu f$ and are purely real when $\mu_e > 0$. Next consider the M, N, P, and Q notation that is similar (but not identical) to Wu and Rosenbaum [7]. By letting $P = \mathrm{Re}\{C_1\}$ and $Q = \mathrm{Im}\{C_1\}$, where $C_1 = \pi(Z_{11} + Z_\circ)/(\psi Z_f)$, we find from the above equations that

$$P = \left(\frac{\pi}{\psi}\right)\left(\frac{Z_\circ}{Z_f}\right) \tag{31}$$

and

$$Q \approx f_{11} - (\ln\psi - 1)f_{11}^a. \tag{32}$$

As for M and N, let $M = \mathrm{Re}\{C_2\}$ and $N = \mathrm{Im}\{C_2\}$, where $C_2 = \pi Z_{31}/(\psi Z_f)$. To satisfy the circulation condition, it follows from Wu and Rosenbaum that $P = M(3N^2 - M^2)/(M^2 + N^2)$ and $Q = N(N^2 - 3M^2)/(M^2 + N^2)$ [7]. It is important to recognize at this point that the right-hand sides of the two previous equations are independent of the coupling angle ψ (under the small angle approximation). Obversely, the function P is inversely proportional to the coupling angle and Q is dependent on ψ in the logarithmic sense. Hence, from (31) and (32), it follows that

$$\psi = \left(\frac{\pi}{P}\right)\left(\frac{Z_\circ}{Z_f}\right) \approx \exp\left(1 + \frac{f_{11} - Q}{f_{11}^a}\right). \tag{33}$$

The previous equation shows the strong dependency of Z_{11} and its asymptotic term on the coupling angle. The equation also allows for a quick first-order design of a circulator and is much easier to implement than the set of equations provided in [7].

III. Numerical Results

Numerical examples pertaining to the calculation of the Green's function $G(\phi, \phi')$ and the Z-parameters are first provided in this section. To establish a meaningful comparison to past research, the parametric values used in this section are taken from Wu and Rosenbaum [7]: $4\pi M_s = 1000$ G, $H_\circ = 0.0$, and $\epsilon_f = 13.0$; the center frequency of operation is chosen to be 10.0 GHz.

The convergence behavior of the original and asymptotically modified Green's functions is compared when $a = 0.254$ cm and for the following two cases: $\phi - \phi' = 0.01$ r (Fig. 2) and $\phi - \phi' = 1.00$ r (Fig. 3). In each of these figures, (2) and (7) are plotted as a function of the azimuthal model index n. As expected, the asymptotically modified Green's function rapidly converges within three to ten terms, regardless of the value of $\phi - \phi'$. Obversely, the Bosma Green's function fails to converge after 100 terms in Fig. 2 and exhibits damped-sinusoidal oscillations about the final solution in Fig. 3 [14]. It is clear from these plots that computations based upon the expression of (2) will be in error if only a few terms are used in the summation.

With the convergence properties of the Green's function understood, we now turn attention to the evaluation of the Z-parameters, which are derived by integrating the Green's function per (13)–(15). This can be accomplished in one of two ways. The first method is by means of analytical approximations that result in the expressions of (16)–(21); the second is by using a Gauss-quadrature technique that accounts for the logarithmic singularity in the integrand, as described by [20]. The results from both of these methods are compared against each other to determine consistency and veracity. For example, consider the

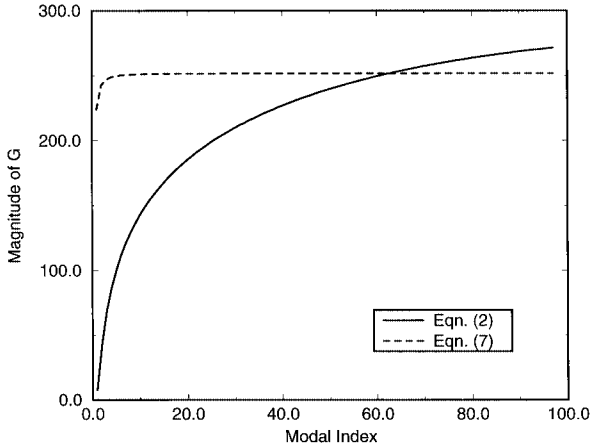

Fig. 2. Convergence data of $G(\phi, \phi')$ as a function of n, as derived from (2) and (7) when $\phi - \phi' = 0.01$ r.

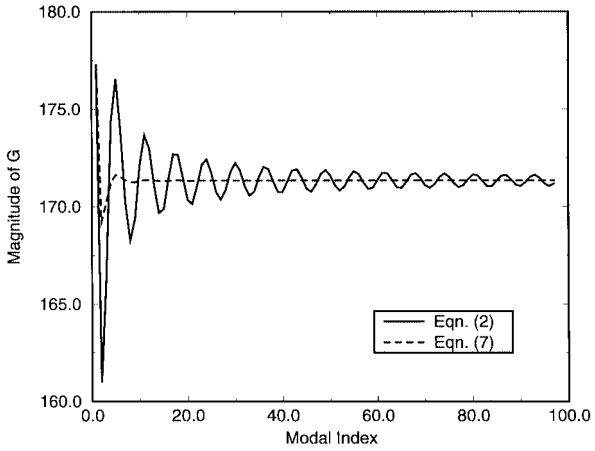

Fig. 3. Convergence data of $G(\phi, \phi')$ as a function of n, as derived from (2) and (7) when $\phi - \phi' = 1.0$ r.

results of Fig. 4, which shows the magnitude of Z_{11} as a function of modal index n when $\psi = 0.3$ r. It is clear from this figure that close correlation between methods is achieved when n exceeds 20. This close correlation of data provides confidence in the closed-form Z-parameter expressions of (16)–(21) and in the approximations used to derive the same.

To conclude this section, an illustrative design example using the small coupling angle formula of (33) is offered, where it is assumed that κ/μ is known at the center frequency of 10 GHz; a constant port impedance of 50 Ω is assumed. (The value of κ/μ is deduced from values of M_s and $H_\circ$ given at the beginning of this section.) Numerical solutions associated with (33) are provided in Table I. Consider the third solution of Table I (i.e., $a = 0.673$ cm and $\psi = 0.0729$ r), which corresponds to a reasonably small coupling angle. Using no approximations, other than those associated with numerical integration, we calculated the S-parameters for this solution; the data are shown in Fig. 5. Also shown in this figure is S_{11} associated with the exact solution of the Wu and Rosenbaum procedure, which is $a = .670$ cm and $\psi = 0.0648$ r. Note, in particular, the close agreement between the two S_{11} data sets. Although the exact

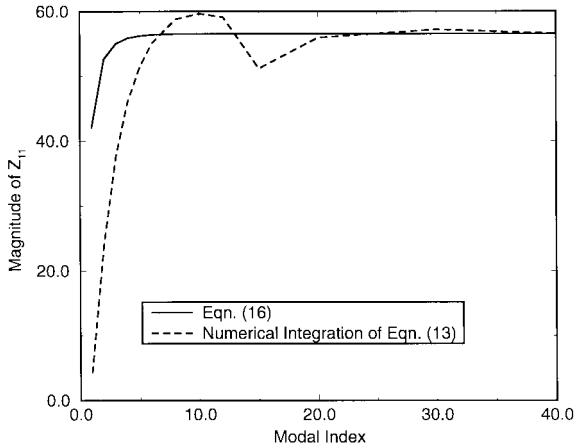

Fig. 4. Plots of Z_{11} as a function when $\psi = 0.3$ r. Comparison is made between data sets associated with analytical approximations and direct numerical integration.

TABLE I
CIRCULATOR DESIGN VALUES

a (cm)	ψ (r)
0.547	0.608
0.594	0.786
0.673	0.0729

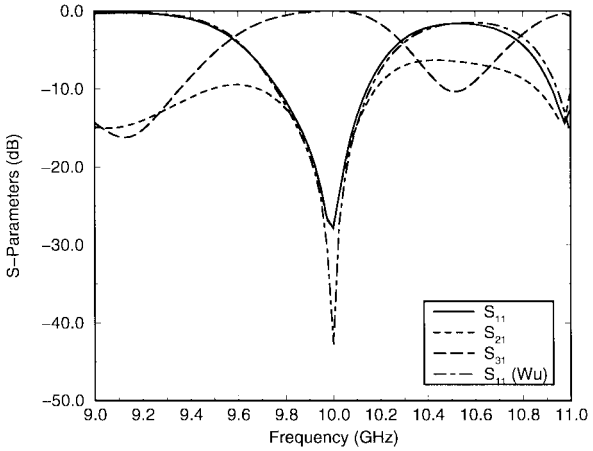

Fig. 5. S_{11}, S_{21}, and S_{31} data sets when $a = 0.673$ cm and $\psi = 0.0729$ r, S_{11} (Wu) data set for $a = .670$ r and $\psi = 0.0678$ r.

solution shows a deeper resonance (i.e., 44 versus 28 dB), both show resonance at 10 GHz.

IV. CONCLUDING REMARKS

In this paper, a comprehensive analysis of the Bosma Green's function has been provided. That analysis has revealed both the convergence rate and singular nature of the Bosma Green's function. With such information, we have developed accurate representations of the circulator's performance metrics, such as the impedance and scattering parameters, and have deduced a simple first-order design formula. Unlike the design procedure of Wu and Rosenbaum [7], this design formula is simple to implement into numerical code and computes rapidly. It is surmised that the design formula of (33) contains important design information with respect to wide-band operation.

APPENDIX

Consider the following integral function:

$$M^{\pm}(\phi) = \int_{(-\pi/(3-\psi))}^{(-\pi/(3+\psi))} \ln\left[1 - e^{\pm j(\phi-\phi')}\right] d\phi' \tag{34}$$

where for purposes of the Z-parameter calculations

$$\phi = \begin{cases} -\dfrac{\pi}{3} & \text{port 1} \\ \dfrac{\pi}{3} & \text{port 2} \\ \pi & \text{port 3.} \end{cases} \tag{35}$$

By definition, $M_{11}^{\pm} = M^{\pm}(-\pi/3)$, $M_{21}^{\pm} = M^{\pm}(\pi/3)$, and $M_{31}^{\pm} = M^{\pm}(\pi)$. Consider first the case when $\phi = -\pi/3$. By means of the equation $u = \phi' + \pi/3$, we may replace (34) with

$$M_{11}^{+} = \int_{-\psi}^{\psi} \ln\left[1 - e^{ju}\right] du. \tag{36}$$

By factoring the term $e^{ju/2}$ from the argument of the logarithmic function and by performing some simple integrations, we obtain

$$M_{11}^{+} = 2\psi \ln 2 + 4 \int_{0}^{(\psi/2)} \ln(\sin u) du. \tag{37}$$

The next step is to recognize that, for typical values of ψ, $\sin u \approx u - u^3/6 = u(1 + u/\sqrt{6})(1 - u/\sqrt{6})$. Hence,

$$M_{11}^{+} \approx 2\psi \ln 2 + 4 \int_{0}^{(\psi/2)} \ln u du + 4 \int_{0}^{(\psi/2)} \ln\left(1 + \frac{u}{\sqrt{6}}\right) du + 4 \int_{0}^{(\psi/2)} \ln\left(1 - \frac{u}{\sqrt{6}}\right) du. \tag{38}$$

Each of the aforementioned integrals can be evaluated using simple techniques of calculus. The final result of those integrations is

$$M_{11}^{+} \approx 2\psi \ln\psi - 6\psi + 4\sqrt{6}\left(1 + \frac{\psi}{2\sqrt{6}}\right) \ln\left(1 + \frac{\psi}{2\sqrt{6}}\right) - 4\sqrt{6}\left(1 - \frac{\psi}{2\sqrt{6}}\right) \ln\left(1 - \frac{\psi}{2\sqrt{6}}\right). \tag{39}$$

By means of similar mathematical operations, it can be shown that $M_{11}^{+} = M_{11}^{-}$.

Even for large coupling angles (i.e., $\psi < 1.0$), we may replace the logarithmic terms with their small argument form (i.e., $\ln(1 \pm x) \approx \pm x$). Upon doing so, we find that

$$M_{11}^{+} \approx 2\psi \ln\psi - 6\psi + 4\sqrt{6}\left(1 + \frac{\psi}{2\sqrt{6}}\right)\left(\frac{\psi}{2\sqrt{6}}\right) + 4\sqrt{6}\left(1 - \frac{\psi}{2\sqrt{6}}\right)\left(\frac{\psi}{2\sqrt{6}}\right). \tag{40}$$

Further manipulation yields

$$M_{11}^{+} \approx 2\psi \ln\psi - 2\psi \tag{41}$$

which would have been the expected result had only the approximation $\sin u \approx u$ in (37) been used.

For the other two cases (i.e., $\phi = \pi/3$ and $\phi = \pi$), a similar procedure to that above can be employed to obtain integral expressions for M_{21}^{+}, M_{21}^{-}, M_{31}^{+}, and M_{31}^{-}. However, given that the integrands of these integrals are not singular within the bounds of the integration limits, but are rather smooth and slowly varying, it behooves us to approximate these integrands using trapezoidal functions [17]. Doing so, we obtain

$$M^{\pm}(\phi) \approx \psi\left\{\ln\left[1 - e^{\pm j(\phi+(\pi/3)-\psi)}\right] + \ln\left[1 - e^{\pm j(\phi+(\pi/3)+\psi)}\right]\right\}. \tag{42}$$

If the coupling angle is small such that $\phi + \pi/3 \gg \psi$ then

$$M^{\pm}(\phi) \approx 2\psi \ln\left[1 - e^{\pm j(\phi+(\pi/3))}\right]. \tag{43}$$

From this expression, it follows that

$$M_{21}^{\pm} \approx \psi\left(\ln 3 \mp j\frac{\pi}{3}\right) \approx \psi(1 \mp j) \tag{44}$$

and

$$M_{31}^{\pm} \approx \psi\left(\ln 3 \pm j\frac{\pi}{3}\right) \approx \psi(1 \pm j). \tag{45}$$

ACKNOWLEDGMENT

The authors express gratitude to Dr. D. Webb, Dr. C. Krowne, and Dr. H. Newman, all of the Naval Research Laboratory (NRL), Washington, DC, for their comments on the theoretical and practical aspects of circular design.

REFERENCES

[1] J. D. Adam, L. E. Davis, G. F. Dionne, E. F. Schloemann, and S. N. Stitzer, "Ferrite devices and materials," *IEEE Trans. Microwave Theory Tech.*, vol. 50, pp. 721–737, Mar. 2002.

[2] H. How, A. Oliver, S. W. McKnight, P. M. Zavracky, N. E. McGruer, C. Vittoria, and R. Schmidt, "Theory and experiment of thin-film junction circulator," *IEEE Trans. Microwave Theory Tech.*, vol. 46, pp. 1645–1653, Nov. 1998.

[3] S. A. Oliver, P. Shi, H. How, S. W. McKnight, N. E. McGruer, P. M. Zavracky, and C. Vittoria, "Integrated self-biased hexaferrite microstrip circulators for millimeter-wavelength applications," *IEEE Trans. Microwave Theory Tech.*, vol. 49, pp. 385–387, Feb. 2001.

[4] H. Bosma, "On stripline Y-circulation at UHF," *IEEE Trans. Microwave Theory Tech.*, vol. MTT-12, pp. 61–72, Jan. 1964.

[5] J. B. Davies and P. Cohen, "Theoretical design of symmetrical junction stripline circulators," *IEEE Trans. Microwave Theory Tech.*, vol. MTT-11, pp. 506–512, Nov. 1963.

[6] C. E. Fay and R. L. Comstock, "Operation of the ferrite junction circulator," *IEEE Trans. Microwave Theory Tech.*, vol. MTT-13, pp. 15–27, Jan. 1965.

[7] Y. S. Wu and F. J. Rosenbaum, "Wide-band operation of microstrip circulators," *IEEE Trans. Microwave Theory Tech.*, vol. MTT-22, pp. 849–856, Oct. 1974.

[8] E. Schloemann and R. E. Blight, "Broad-band stripline circulators based on YIG and Li-ferrite single crystals," *IEEE Trans. Microwave Theory Tech.*, vol. MTT-34, pp. 1394–1400, Dec. 1986.

[9] R. E. Neidert and P. M. Phillips, "Losses in Y-junction stripline and microstrip circulators," *IEEE Trans. Microwave Theory Tech.*, vol. 41, pp. 1081–1086, June 1993.
[10] H. How, C. Vittoria, and R. Schmidt, "Losses in multiport stripline/microstrip circulators," *IEEE Trans. Microwave Theory Tech.*, vol. 46, pp. 543–545, May 1998.
[11] C. M. Krowne, "Electromagnetic conductor loss inclusion method in self-consistent 2D Green's function solver for inhomogeneous microstrip circulator," *Int. J. Numer. Model.*, vol. 12, pp. 399–415, 1999.
[12] H. S. Newman and C. M. Krowne, "Analysis of ferrite circulators by 2-D finite-element and recursive Green's function techniques," *IEEE Trans. Microwave Theory Tech.*, vol. 46, pp. 167–177, Feb. 1998.
[13] C. M. Krowne and R. E. Neidert, "Theory and numerical calculations for radially inhomogeneous circular ferrite circulators," *IEEE Trans. Microwave Theory Tech.*, vol. 44, pp. 419–431, Mar. 1996.
[14] C. M. Krowne, "Theory of the recursive dyadic Green's function for inhomogeneous ferrite canonically shaped microstrip circulators," in *Advances in Imaging and Electron Physics*, Peter W. Hawkes, Ed. New York: Academic, 1996, vol. 98, pp. 77–321.
[15] ——, "Anisotropic recursive dyadic Green's function 3D theory for a radially inhomogeneous microstrip circular ferrite circulator," *Int. J. Numer. Model.*, vol. 12, pp. 355–387, 1999.
[16] D. Polder, "On the theory of ferromagnetic resonance," *Phil. Mag.*, vol. 40, pp. 99–115, 1949.
[17] M. Abramowitz and J. E. Stegun, *Handbook of Mathematical Functions With Formulas, Graphs and Mathematical Tables*. Washington, DC: U.S. Gov. Printing Office, 1970.
[18] S. Singh, W. F. Richards, J. R. Zinecker, and D. R. Wilton, "Accelerating the convergence of series representing the free space periodic Green's function," *IEEE Trans. Antennas Propagat.*, vol. 38, pp. 1958–1962, Dec. 1990.
[19] A. D. Wheelon, *Tables of Summable Series and Integrals Using Bessel Functions*. San Francisco, CA: Holden-Day, 1968.
[20] A. F. Peterson, S. L. Ray, and R. Mittra, *Computational Methods for Electromagnetics*. Piscataway, NJ: IEEE Press, 1998.

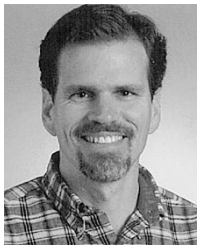

Jeffrey L. Young (S'79–M'89–SM'00) received the B.S.E.E. degree from Ohio Northern University, Ada, in 1981, and the M.S.E.E. and Ph.D. degrees from the University of Arizona, Tucson, in 1984 and 1989, respectively.

He was a Doctoral Fellow and Staff Engineer with the Hughes Aircraft Company. He is currently a Professor of electrical and computer engineering at the University of Idaho, Moscow. His research interests include electrooptical modulation, ferrite microwave devices, electromagnetic-wave propagation in complex media, and modern numerical methods in electromagnetics.

Dr. Young was an editor of the *IEEE Antennas and Propagation Magazine* for nine years. He is currently an elected member of the IEEE Antennas and Propagation Society (IEEE AP-S) Administrative Committee. He is a member of URSI (Commission B).

James W. Sterbentz received the M.S.N.E. and B.S.N.E./B.S.M.E. degrees from the University of California at Berkeley, in 1978 and 1977, respectively, and the Ph.D. degree in nuclear engineering from Oregon State University, Corvallis, in 1983.

He is currently an Advisory Engineer with the Idaho National Engineering and Environmental Laboratory (INEEL), Idaho Falls, ID, where he directs research in the design of advanced generation IV nuclear reactors. His interest in electrical engineering, particularly electromagnetic-wave propagation phenomena, has led to graduate study research in the design and analysis of microwave circulator devices.